Co-optimizing Energy Storage for Prosumers using Convex Relaxations

Md Umar Hashmi*, Deepjyoti Deka†, Ana Bušić*, Lucas Pereira‡, and Scott Backhaus†
* INRIA and Ecole Normale Supérieure, CNRS, PSL Research University, Paris, France
† Los Alamos National Laboratory, the USA
‡ Madeira-ITI, Ténico Lisboa, and prsma.com, Madeira, Portugal

***Abstract*—This paper presents a new co-optimization formulation for energy storage for performing energy arbitrage and power factor correction (PFC) in the time scale of minutes to hours, along with peak demand shaving in the time scale of a month. While the optimization problem is non-convex, we present an efficient penalty based convex relaxation to solve it. Furthermore, we provide a mechanism to increase the storage operational life by tuning the cycles of operation using a friction coefficient. To demonstrate the effectiveness of energy storage performing multiple tasks simultaneously, we present a case study with real data for a time scale of several months. We are able to show that energy storage can realistically correct power factor without significant change in either arbitrage gains or peak demand charges. We demonstrate a real-time Model Predictive Control (MPC) based implementation of the proposed formulation with AutoRegressive forecasting of net-load and electricity price. Numerical results indicate that arbitrage gains and peak demand shaving are more sensitive to parameter uncertainty for faster ramping battery compared to slower ramping batteries. However, PFC gains are insensitive to forecast inaccuracies.**

I. Introduction

In today's smart grid, many electricity consumers also generate part of their consumed electricity locally using renewable energy sources. Such consumers are referred to as electricity *prosumers*. Active participation of low voltage prosumers in electricity markets can lead to mutual benefits for both the utility as well as reduced costs for the prosumers [1], [2]. While renewable energy sources are clean and cheap, they are also intermittent and hence unreliable. In this context, energy storage devices such as batteries present a good alternative to act as a buffer and reduce the energy fluctuations due to renewables.

TABLE I
Energy storage applications and time-scales

Storage Application	Time scale
(1.) Frequency regulation	milliseconds to few sec.
(2.) Ancillary services	seconds to few minutes
(3.) Energy Arbitrage	minutes to hours
(4.) Power factor correction	minutes to hours
(5.) Peak demand reduction	days to months

While energy storage devices can act as a technology enabler for power systems, they are still expensive and often not financially viable for use in a specific application alone [3] in both North American and European energy markets. It is thus necessary to combine various roles for operating energy storage for profitability as shown in the pioneering work [4]. Authors in [5] observe that multi-tasking of storage devices leads to a significant reduction in total losses and reduce environmental impacts. However, a major challenge with co-optimizing for multiple applications is in dealing with *different revenue streams* and penalties with *differing time scales* of operation. Table I lists a non-exhaustive list of roles energy storage can perform and time scales at which these roles operate.

Fast operations in ancillary services requires commitment of services prior to participation and correct responsiveness to control signals [6], [7]. Lack of communication/monitoring equipment make it extremely difficult for low voltage (LV) electricity consumers to participate in dynamic regulation. Therefore, in this work we focus on co-optimizing the following storage applications for LV distribution grid prosumers in the time-scale of minutes to several days for performing:

• **Energy Arbitrage**: End-users can charge their batteries when prices are low and discharge when prices are high and in effect reduce their electricity bills [8].

• **Peak Demand Charge**: Many power utilities around the world have introduced charges for peak demand [9]–[11] that a consumer may seek to minimize over a longer period (weeks or months).

• **Power Factor Correction** (PFC): Distributed generation (DG) often operate at close to unity power factor as they are not obliged to supply reactive power. In this work, we assume electricity consumer is *obliged* to maintain a power factor (PF) magnitude greater than or equal to a threshold set by the utility.

Multiple works in the past have looked at individual battery goals. [8], [12] have analyzed the use of batteries in arbitrage. The authors in [13] use energy storage for peak demand shaving for industrial loads, while [14], [15] present peak shaving in the context of residential electricity consumers. PFC using energy storage converter is presented in [16], [17]. While such correction is currently mandated for large consumers [18], PFC for domestic customers may be mandated in the near future. Co-optimization of energy storage usage is a growing work of research. [4], [19], [20] discusses storage utilization for arbitrage and frequency regulation, while [21] analyzes phase balancing along with arbitrage. Similarly, peak shaving has been co-optimized with frequency regulation in [22], [23]

978-1-7281-3192-4/19/$31.00 ©2019 IEEE

and with arbitrage and energy backup in [24] along with increasing self-sufficiency in [25]. Prior work on co-optimization problems for different time-scale applications such as [22], [23] do not explicitly propose a split of optimization horizon between the different time scales. In our work, we overcome this by an efficient split.

Contribution: In this work, we focus on co-optimizing energy storage across multiple time-scales for performing energy arbitrage, peak demand shaving and power factor correction (PFC). The inclusion of power factor correction makes the joint optimization problem non-convex, but we solve it efficiently using a penalty-based convex-relaxation scheme inspired by our prior work on *single* time-scale battery optimization for arbitrage and PFC [16]. To include the peak demand charge with *longer* time-scales, we use a memory variable that enables us to split the longer optimization problem into smaller sections for an efficient solution. Finally, we account for battery degradation into our formulation by introducing friction coefficient to control battery cycles. We present simulation results using 80 days of real load data from Madeira, Portugal with real-time electricity price data from CAISO and peak demand charge from PG&E in California. To account for real-time application, we consider a Model Predictive Control (MPC) framework where AutoRegressive forecasting is used to predict future prices and loads. The overarching conclusion of our work is that energy storage devices can significantly raise profits by co-optimizing multi time-scale goals without any deterioration in individual gains. For the real-time implementation, peak demand shaving and arbitrage gains are affected by uncertainty modeling for batteries with faster ramp rates, though PFC is not sensitive.

The next section presents the system description. Section III formulates co-optimization problem for performing arbitrage, PF correction and peak demand charge saving. Section IV presents an online implementation of the co-optimization formulation presented in an MPC setting with autoregressive forecasting. Section V presents the numerical results. Section VI concludes the paper.

II. System Description

In this work, we consider a LV electricity consumer with inelastic demand, rooftop solar generation and a battery, as shown in Fig. 1. We denote time instant as a superscript

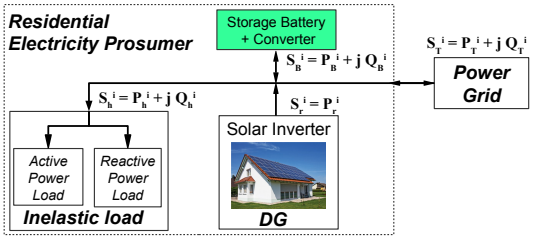

Fig. 1. Electricity prosumer block diagram with DG and storage

of the variable. The time horizon T is divided into N steps indexed by $\{1, ..., N\}$. The sampling time is denoted as h, thus $T = hN$. The apparent power of the load, solar generation and battery is shown in Fig. 1, at i^{th} time instant. The apparent power of the inelastic load, S_h^i, is the sum of its active power, P_h^i, and reactive power, Q_h^i. The solar inverter operates at unity power factor, thus its apparent power S_r^i is equal to its active power P_r^i. The net load of the prosumer is the combination of its inelastic load and renewable generation. Its active power is denoted as $P^i = P_h^i - P_r^i$. Similarly, the total reactive power of the prosumer is denoted as $Q^i = Q_h^i$. We assume that the prosumer settles its electricity bill every month. The number of decision samples in a month is denoted as N_{month}. Next we discuss the battery model.

A. Battery Model

The storage is interfaced via converter (rectifier during charging or inverter during discharging) and can supply active and reactive power. The apparent power output of energy storage converter is given as $S_B^i = P_B^i + jQ_B^i$, where P_B^i, Q_B^i denote active and reactive power outputs respectively. The battery model used takes into account the ramping and the capacity constraint and the efficiency losses. At time i, the change in the energy level is denoted as x^i. If $x^i > 0$, it implies battery is charging and vice versa. The ramp rate of the battery is denoted as x^i/h. The ramp rate should satisfy $x^i/h \in [\delta_{\min}, \delta_{\max}]$, where $\delta_{\min}$ denotes the minimum ramp rate (kW), and $\delta_{\max}$ denotes the maximum ramp rate (kW). The charging and discharging efficiencies of the battery are denoted as $\eta_{ch}, \eta_{dis} \in (0, 1]$, respectively. The battery active power, denoted as P_B^i, is given as

$$P_B^i = \frac{[x^i]^+}{h\ \eta_{ch}} - \frac{[x^i]^- \eta_{dis}}{h}. \tag{1}$$

Based on the definition of P_B^i in Eq. 1, the active power constraint is given by

$$P_B^i \in [P_B^{\min}, P_B^{\max}] = [\delta_{\min}\eta_{dis}, \frac{\delta_{\max}}{\eta_{ch}}]. \tag{2}$$

The converter rating is given by maximum apparent power supplied/consumed and denoted as $S_B^{\max}$. The instantaneous apparent power of battery S_B^i should satisfy the converter rating, and is constrained as

$$(S_B^{\max})^2 \geq (S_B^i)^2 = (P_B^i)^2 + (Q_B^i)^2. \tag{3}$$

The reactive power (Q_B^i) output of the battery converter is thus constrained by converter rating and instantaneous active power output. The energy stored in the battery at the i^{th} step is given as $b^i = b^{i-1} + x^i$. The battery energy is made to follow the capacity constraint given as

$$b^i \in [b_{\min}, b_{\max}]\ \forall i \tag{4}$$

where $b_{\min}$ and $b_{\max}$ denote minimum and maximum battery charge level respectively. The total active power including storage output is given as $P_T^i = P_h^i - P_r^i + P_B^i$ and the total reactive power is $Q_T^i = Q_h^i + Q_B^i$, as shown in Fig. 1.

B. Power Factor Correction (PFC) with Battery

We define the uncorrected power factor as the PF seen by the grid in absence of energy storage and is given as $\text{pf}^i_{\text{bc}} = P^i/\sqrt{P^{i2} + Q^{i2}}$. Since solar inverter operates at unity power factor during the day, the power factor seen by the grid deteriorates. With the inclusion of storage, power factor takes the following form $\text{pf}^i_{\text{c}} = P^i_T/\sqrt{(P^i_T)^2 + (Q^i_T)^2}$. To keep the power factor from deteriorating outside the permissible bounds, the following constraint should be satisfied

$$-k \leq Q^i_T/|P^i_T| = (Q^i + Q^i_B)/|P^i + P^i_B| \leq k, \quad (5)$$

where $k = \tan(\theta_{\min})$. The assumption on identical limits in Eq. 5 can be easily generalized for unequal leading and lagging PF magnitudes. Next we discuss the billing structure considered in this paper.

C. Billing Structure

We consider the variable cost of electricity to consist of three components. In our setting, each component has a value which automatically either blocks or prioritizes certain application, unlike [26] which prioritizes storage application. For instance, if ramping up for arbitrage is more profitable in certain time instant compared to peak shaving then the battery should ramp up. The three components are

(1) *Active energy cost*: equals the product of time varying cost of electricity denoted as p^i_{elec} and the amount of active energy consumed, is denoted as

$$C^i_P = p^i_{\text{elec}} \times P^i_T h. \quad (6)$$

(2) *Reactive energy cost/ PF penalty*: denoted as

$$C^i_Q = \lambda \max\left(0, \left|Q^i_T\right| - k\left|P^i_T\right|\right), \quad (7)$$

here λ denotes the penalty for reactive power if the PF dips below the limit prescribed. The mechanism for pricing reactive energy in Eq. 7 has similarities with charges imposed by UTE (Uruguay's government-owned power company) [27] and PF limits and penalty listed in Table II, see [16].

TABLE II
POWER FACTOR RULES

Utility/Country	PF Limit	Reactive Cost
France [28]	$\lvert\tan(\phi)\rvert \leq 0.4$	$0.2 \times C^i_P$
Portugal [29]	$\lvert\cos(\phi)\rvert \geq 0.92$	0.016 to 0.18 $\times C^i_P$
Germany [30]	$\lvert\cos(\phi)\rvert \geq 0.95$	for Solar Generators
CAISO	$\lvert\cos(\phi)\rvert \geq 0.85$	LV consumers [31]

(3) *Peak demand cost*: denoted as

$$C_{peak} = \lambda_{\text{peak}} \max\left(P^i_T, \forall i \in \{1, ..., N_{\text{month}}\}\right), \quad (8)$$

where the maximization is over a month. λ_{peak} denotes the peak-demand charge imposed on a time-scale of a month. The total variable cost of electricity for a month is given as

$$C^{\text{month}}_T = C_{peak} + \sum_{i=1}^{N_{\text{month}}} \left\{C^i_P + C^i_Q\right\}. \quad (9)$$

III. CO-OPTIMIZATION OF ENERGY STORAGE

In this section we formulate the problem for co-optimizing arbitrage, PFC and peak demand shaving.

A. Energy Arbitrage

Arbitrage refers to procurement under low prices and sale under high prices. Energy storage arbitrage considers the time-variation of net consumer load and electricity price p^i_{elec}. We assume the buying and selling prices at each time to be same. Under such a case, the storage operation depends only on the price and is independent of the inelastic load and renewable generation [3], [32]. Since the monetary benefits from energy arbitrage is *based only on* active power output, the prosumer minimizes the following problem

$$(P_{arb}) \min_{P_B, Q_B} \sum_{i=1}^{N} p^i_{elec} P^i_B h, \quad \text{subject to, Eq. 2, Eq. 3, Eq. 4.} \quad (10)$$

B. Arbitrage with PFC

The cost function for co-optimizing PFC and arbitrage, introduced in [16], is denoted as P_{plt} and is given by

$$\min_{P_B, Q_B} \quad \sum_{i=1}^{N} \left\{p^i_{elec} P^i_B h + C^i_Q\right\}. \quad (11)$$

C^i_Q in Eq. 7 comes from Eq. 7 and denotes the PF penalty. We can model it as:

$$C^i_Q \geq 0, \quad C^i_Q \geq \lambda(|Q^i_T| - k|P^i_T|). \quad (12)$$

Here the mod or absolute value $|x|$ is represented in a mixed-integer form as $(2z-1)x \geq 0$. z is a binary variable that takes a value of 1 for $x > 0$ and 0 otherwise. Eq. 12 can now be reformulated as

$$\begin{aligned} &C^i_Q \geq 0, \quad C^i_Q \geq \lambda(2y^i_1 - Q^i_T - 2ky^i_2 + kP^i_T). \\ &2y^i_1 - Q^i_T \geq 0, \quad 2y^i_2 - P^i_T \geq 0 \end{aligned} \quad (13)$$

Here y^i_1 and y^i_2 denote bi-linear variables defined as

$$y^i_1 = z^i_1 Q^i_T, \quad y^i_2 = z^i_2 P^i_T \quad (14)$$

with binary variables z^i_1 and z^i_2. z^i_1 (z^i_2) takes a value of 1 when the net reactive (active) power is positive, otherwise it takes a value equal to zero. We use McCormick relaxation [33] to convert the bi-linear terms in Eq. 14 to mixed-integer linear constraints.

$$\begin{aligned} &y^i_1 \geq Q^i_{lb} z^i_1, \quad y^i_1 \geq Q^i_T + Q^i_{ub} z^i_1 - Q^i_{ub} \\ &y^i_1 \leq Q^i_{ub} z^i_1, \quad y^i_1 \leq Q^i_T + Q^i_{lb} z^i_1 - Q^i_{lb} \\ &y^i_2 \geq P^i_{lb} z^i_2, \quad y^i_2 \geq P^i_T + P^i_{ub} z^i_2 - P^i_{ub} \\ &y^i_2 \leq P^i_{ub} z^i_2, \quad y^i_2 \leq P^i_T + P^i_{lb} z^i_2 - P^i_{lb}. \end{aligned} \quad (15)$$

In these equations, $P^i_{lb} = P^i + P^{\min}_B$, $P^i_{ub} = P^i + P^{\max}_B$, $Q^i_{lb} = Q^i - S^{\max}_B$ and $Q^i_{ub} = Q^i + S^{\max}_B$ denote the lower and upper bounds for total active and reactive power. As the bilinear terms include a binary variable, the McCormick relaxations are known to be exact. The optimization problem for performing arbitrage with power factor penalties is given below.

$$(P_{plt}) \quad \min_{P_B, Q_B} \quad \sum_{i=1}^{N} \left\{p^i_{elec} P^i_B h + C^i_Q\right\} \quad (16)$$

subject to, Eq. 2, Eq. 3, Eq. 4, Eq. 13, Eq. 15.

C. Peak Demand Shaving with PFC and arbitrage

We now add peak demand charge λ_{peak} (per units of power) to the formulation. The total cost is proportional to the peak electricity demand over a longer period of time (1 month) unlike P_{arb} and P_{plt}. However, we split the optimization horizon to one day interval using a memory variable to make the problem tractable as below.

$$(P_{plt}^{\text{peak}}) \min_{P_B, Q_B} \sum_{i=1}^{N} \left\{ p_{\text{elec}}^i P_B^i h + C_Q^i + \lambda_{\text{peak}} \max(P_T^i, P_{\max}^{\text{previous}}) \right\} \tag{17}$$

subject to, Eq. 2, Eq. 3, Eq. 4, Eq. 13, Eq. 15.

Variable $P_{\max}^{\text{previous}}$ here acts as the memory of peak loads in the previous days of the month. The $P_{\max}^{\text{previous}}$ is initialized, and updated if the peak power exceeds the current value. The overall optimization and update steps are shown in Algorithm 1. In order to obtain results not biased because of initialization of memory variable, we select it as zero at the beginning of each month. In practical implementation we advice to initialize $P_{\max}^{\text{previous}}$ with more realistic functions of historical peak load and storage ramp rate. Other combinations of co-optimization (for example arbitrage with peak shaving) can be formed by dropping the unused functions (related to PFC).

D. Co-optimization with control of cycles

Note that the formulations discussed previously do not consider battery life that is affected by charge-discharge cycles. Battery manufacturers measure the life of a battery using two indices: cycle life and calendar life. Cycle life denotes the number of cycles a battery can operate at a certain depth-of-discharge before reaching its end-of-life or EoL[1]. Similarly, calendar life denotes the maximum probable age that the battery can be operational before reaching EoL. Following our prior work [34], we define a friction function for the active power to model the degradation due to cycles of operation as $P_{\text{fric}}^i = \frac{[P_B^i]^+}{\eta_{\text{fric}}} - [P_B^i]^- \eta_{\text{fric}}$, here η_{fric} denotes the friction coefficient. The new optimization function is given as

$$(P_{cyc}) \min_{P_B, Q_B} \sum_{i=1}^{N} \left\{ p_{\text{elec}}^i P_{\text{fric}}^i h + C_Q^i + \lambda_{\text{peak}} \max(P_T^i, P_{\max}^{\text{previous}}) \right\} \tag{18}$$

subject to, Eq. 2, Eq. 3, Eq. 4, Eq. 13, Eq. 15.

The friction coefficient takes a value from 1 to 0. η_{fric} needs to be tuned so as the operational life is increased by matching calendar and cycle degradation of the battery [35]. If the battery is not over operating then η_{fric} is set to 1. For cases where the battery is performing more cycles, the low returning transactions could be eliminated by decreasing the value of η_{fric}. Note that the control of cycles is only imposed on the arbitrage component of the objective function, as majority of cycles are performed for arbitrage. We would like to highlight that reactive power depends on converter size and does not affect storage cycles.

[1]EoL is the state of the battery when the maximum battery capacity reduces to 80% of its initial rated capacity in watt-hours.

Algorithm 1 `PeakDemandThresholdUpdate`

Inputs: $\eta_{\text{ch}}, \eta_{\text{dis}}, \delta_{\max}, \delta_{\min}, b_{\max}, b_{\min}, S_B^{\max}, h, N, b_0$,
Initialize: $P_{\max}^{\text{previous}} = 0$

```
while days < Month do
    for i = 1 : N do
        Implement P_plt^peak for the day and find P_T^i,
        P_max^previous = max(P_T^i, P_max^previous),
        Update battery capacity,
    end for
    Update b_0 and increment days = days +1
end while
```

IV. Real-time implementation

In real-world accurate information of parameters such as consumer load and renewable generation for future time is not known. For real-time implementation, we propose to implement the optimization algorithm in a model predictive framework with auto-regressive forecasting described next.

A. AutoRegressive Forecasting

Consider the number of decision samples in a month is denoted as N_{month}. At time k a rolling horizon forecast of N_{opt} number of samples is performed. We present a generalized ARMA model in terms of variable V, that is used for forecasting active power, reactive power and electricity price. We define the mean behavior of past values of V at time step i as

$$\bar{V}^i = \frac{1}{D} \sum_{p=1}^{D} V_{(i-pN_{opt})} \quad \forall i \in \{k, ..., N_{opt}\}, k \geq 1, \tag{19}$$

where N_{opt} denotes the number of points in the optimization horizon of a single day. D denotes the past days which are utilized for calculating the mean $\bar{V}$. Let $\hat{M}^i$ be the difference between V and its mean $\bar{V}$. The forecast $\hat{V}$ is given by

$$\hat{V}_i = \bar{V}_i + \hat{M}_i \quad \forall i \in \{k, ..., N_{opt} + k - 1\}, k \geq 1, \tag{20}$$

We define $\hat{M}_i \quad \forall i \in \{k, ..., N_{opt} + k - 1\}$ as

$$\hat{M}_k = \sum_{j=1}^{J} \alpha_j M_{k-j} + \sum_{u=1}^{U} \beta_u \delta_k^u, \tag{21}$$

where $\delta_k^m = (V_{k-mN} - \bar{V}_{k-mN})$ and $\alpha_i, \beta_i \forall i \in \{1, ..., U\}$ are constants. The weights used in ARMA model, $\alpha_j \forall j \in \{1, ..., J\}, \beta_u \forall u \in \{1, ..., U\}$, are tuned by solving Eq. 22

$$\min \sum_i \{||V_i - \hat{V}_i||^2 + ||\text{norm}([\alpha^i, \beta^i])||^1\}. \tag{22}$$

B. Model Predictive Control

Using historical data, we train ARMA models, one each for active and reactive power, as well as for prices. Using the tuned coefficients, the forecast vectors are identified using Eq. 20 for a horizon with N_{opt} equal to the number of samples in one day. We then feed these forecast vectors a MPC algorithm to determine the optimal energy storage action for time step i. This process is repeated for $i \in \{k+1, ..., N_{\text{opt}} + k\}$, till the end of time horizon is reached. The real-time algorithm is presented in Algorithm 2.

Algorithm 2 `CoOptimizationForecastMPC`

Storage Parameters: $\eta_{\text{ch}}, \eta_{\text{dis}}, \delta_{\max}, \delta_{\min}, b_{\max}, b_{\min}, b_0$.
Inputs: $h, N, T, i = 0$, Rolling horizon optimization time period N_{opt}, Historical load, renewable generation and price data, N_{month}.
Initialize: $P_{\max}^{\text{previous}} = 0$.

1: Use historical data to tune ARMA models for active power, reactive power and electricity price,
2: **while** $i < N_{month}$ **do**
3: Increment $i = i + 1$ and receive $p_{\text{elec}}(i)$ and load P_i, Q_i,
4: Forecast N_{opt} samples of $\hat{P}, \hat{Q}, \hat{p}_{elec}$ using ARMA,
5: Implement P_{plt}^{peak} for the rolling horizon and find P_T^i,
6: Calculate $P_{\max}^{\text{previous}} = \max(P_T^i, P_{\max}^{\text{previous}})$,
7: ${b_i}^*={b^{i-1}}+\hat{x}^*(1)$ s.t. $\hat{x}^*(1)=[{P_B}^*(i)]^+\eta_{\text{ch}}-[{P_B}^*(i)]^-/\eta_{\text{dis}}$,
8: Update $b_0 = {b_i}^*$, the initial capacity of battery is updated,
9: Return ${b^i}^*$, ${P_B}^*(i)$, ${Q_B}^*(i)$.
10: **end while**

V. Numerical Results

In this section, we demonstrate the performance of our optimization formulations through numerical simulations with real data. We consider multiple storage control policies are: (a) P_{arb}: Only arbitrage, (b) P_{plt}: Arbitrage + PFC, (c) P_{plt}^{peak}: Arbitrage + PFC+ Peak demand shaving, (d) P_{pd}: Only peak demand shaving, (e) P_{arb}^{peak}: Arbitrage + Peak demand shaving. P_{cyc} with battery degradation is discussed subsequently. To demonstrate the performance of our algorithms, we use different performance indexes that are listed next.

1) *Arbitrage Gains* G_{arb}: measures effectiveness in performing arbitrage,
2) *Power Factor Correction:* is gauged using *No. of PF violations*, using a prescribed PF limit of 0.9. Gains made by PFC with respect to the nominal case is denoted as G_{reac},
3) Peak Demand Charge Savings (G_{pd}): Consider ΔP_{max} as the reduction in peak demand due to energy storage then the saving is given as $G_{pd} = \lambda_{\text{peak}} \Delta P_{max}$.
4) *Total Gains* G_T: is the sum of arbitrage gains, reactive compensation gains and peak demand charge saving, calculated with respect to nominal,
5) *Converter Usage Factor* (CUF), introduced in [16], equals $\text{CUF} = \frac{1}{N}\sum_{i=1}^{N} \frac{\sqrt{(P_B^i)^2+(Q_B^i)^2}}{S_B^{\max}}$,
6) *Gains per cycle*: Calculated based on equivalent 100% Depth of Discharge (DoD) cycles. We consider the storage degradation model and algorithm to identify equivalent 100% DoD presented in [34].

TABLE III
Battery Parameters

$B_{\min}, B_{\max}, B_0$	200Wh, 2000 Wh, 1000 Wh
$\eta_{\text{ch}} = \eta_{\text{dis}}$	0.95
$\delta_{\max} = -\delta_{\min}$	1000 W for 0.5C-0.5C, 2000 W for 1C-1C 4000 W for 2C-2C,
Cycle Life Calendar Life	4000 cycles at 100% DoD 10 years

For simulation results we consider a period of 80 days starting from 1st of June 2018 and use inelastic load and renewable generation data collected at Madeira, an island in Portugal. The price data for our simulations is taken from CAISO for the same dates [36]. We use PG&E peak demand rate which is \$0.01826/ watt [9]. The gain λ for penalty function $\theta(i)$ is set to be equal to 0.4. The sampling time of our numerical experiment is 5 minutes (288 samples in a day).

Under the *nominal case* for the 80 day period, i.e., without any storage, the consumer pays \$207.88 for active energy, \$46.485 for reactive energy, and \$246.138 for peak demand, and incurs 2894 PF violations. We use these values to calculate gains listed in Table IV.

We use three batteries with different ramping capabilities for comparison. Their parameters are listed in Table III. Battery model is denoted as xC-yC, which implies that the battery takes 1/x hours to charge completely and 1/y hours to discharge completely. Fixing the total energy and varying ramping capability provides a sensitivity analysis of different ramping storage technologies. For computing storage profitability, we consider the 2 kWh battery to have a cost of \$1000, approximately proportional to the cost of Tesla Powerwall per kWh [37]. For the battery given in Table III, each 100% DoD cycle should make more that \$0.2 in order to reach break-even, else this battery will not be profitable.

Fig. 2 shows the variation of nominal peak demand for each day along with $P_{\max}^{\text{previous}}$ for different battery models. It is clear that higher ramping battery can lower the peak demand up to a greater extent.

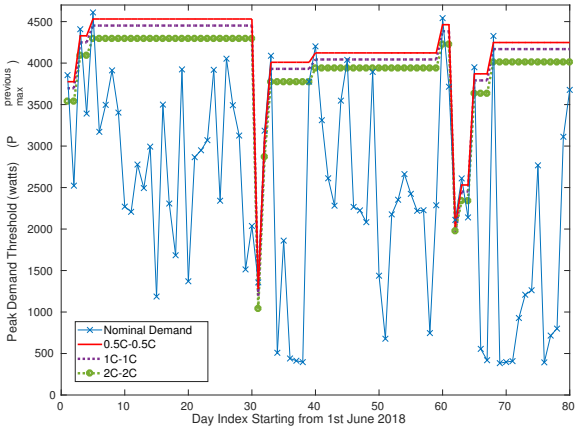

Fig. 2. Variation of $P_{\max}^{\text{previous}}$ as the days progress

Table IV lists detailed results comparing performance indices for different optimization problems and for different battery models. We wish to highlight that performing arbitrage with or without PFC, but without peak shaving can significantly increase peak demand charge that overshadows the marginal extra gain from performing arbitrage alone. This observation is in sync with conclusions drawn by the authors in [22]. More significant are the results for P_{plt}^{peak}. Notice that for different batteries, it is able to reduce PF violations to as much as P_{plt}, while maintaining gains similar to ones in P_{arb}, P_{arb}^{peak}. This highlights the ability of batteries to do PFC over and above arbitrage and peak shaving. Table IV also lists that

TABLE IV
PERFORMANCE INDICES FOR CONVERTER $S_B^{\max} = P_B^{\max}$

Perf.Index	P_{arb}	P_{plt}	P_{plt}^{peak}	P_{pd}	P_{arb}^{peak}
Battery 2C-2C					
PF viol.	3260	11	11	2758	3259
G_{pd} ($)	0.288	0.288	17.347	17.347	17.347
G_{arb} ($)	42.787	42.767	42.751	*−12.756*	42.771
G_{reac} ($)	*−6.731*	46.479	46.479	2.113	*−6.636*
G_T ($)	36.344	89.534	**106.577**	6.704	53.482
Cycles	806.54	803.34	803.85	17.19	807.04
$/cycle	0.0451	0.1115	0.1326	0.3900	0.0663
CUF %	42.67	57.68	57.68	5.46	42.7
Battery 1C-1C					
PF viol.	3058	51	51	2811	3057
G_{pd} ($)	5.782	5.782	8.674	8.674	8.674
G_{arb} ($)	26.349	26.267	26.260	*−6.380*	26.342
G_{reac} ($)	*−4.060*	45.546	45.546	1.020	*−4.021*
G_T ($)	28.071	77.595	**80.48**	3.314	30.995
Cycles	453.90	451.32	451.57	8.11	454.24
$/cycle	0.0618	0.1719	0.1782	0.4086	0.0682
CUF %	49.76	74.16	74.19	5.44	49.80
Battery 0.5C-0.5C					
PF viol.	3024	236	237	2839	3024
G_{pd} ($)	4.337	4.337	4.337	4.337	4.337
G_{arb} ($)	15.404	15.103	15.103	*−3.189*	15.401
G_{reac} ($)	*−1.028*	41.058	41.058	0.529	*−1.006*
G_T ($)	18.713	60.498	**60.498**	1.677	18.732
Cycles	249.93	247.07	247.19	5.09	250.13
$/cycle	0.0749	0.2449	0.2447	0.3295	0.0749
CUF %	56.45	81.61	81.54	5.61	56.49

PF violations decrease with increased ramping. The low CUF for batteries performing only peak demand saving indicates their under-utilization. Hence dedicating storage application only for peak-demand is sub-optimal. To better elucidate the financial gains, we present Fig 3.

From Table IV it is clear that total gains increases significantly with decrease in charge-discharge time. This implies that financial potential of energy storage will increase significantly with faster batteries. Moreover, the storage device performs too many cycles and hence achieves low gains per cycle. For example, the 2C-2C battery operates 806 cycles of 100% DoD cycles in $\approx$ 3 month period, which is equivalent to greater than 20% of its operational life. This motivates the use of P_{cyc} and inclusion of battery life into the model as discussed next.

A. Controlling and Tuning Cycles of Operation

In order to have an operational life equal to calendar life, the battery should operate 400 100% DoD cycles in a year. For our numerical simulation of $\approx$ 3 months, the battery should perform approximately 100 cycles (of 100% DoD). Depending on the storage model, the number of cycles of operation can be tuned using the friction coefficient.

Table V presents gains for different batteries for the friction coefficient at which their calendar life degradation approximates cycle life degradation. Note that for the faster ramping batteries, CUF is quite low. This implies that a smaller converter may be sufficient. Selection of optimal converter based on battery life-cycle is an objective of our future work in this domain.

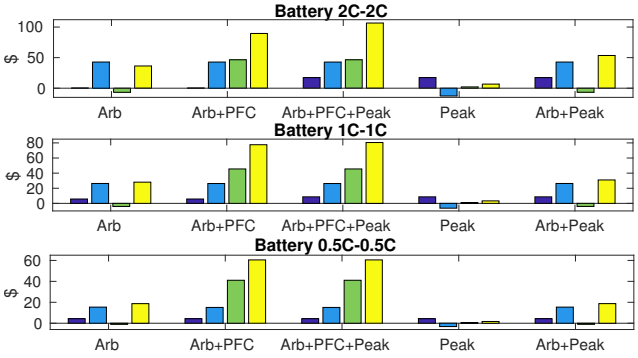

Fig. 3. Gain plot: G_{pd}, G_{arb}, G_{reac}, G_T are shown as four bar

TABLE V
TUNE η_{FRIC}: MATCH CALENDAR AND CYCLE DEGRADATION

Battery	η_{fric}	G_T	cycles	$/cycles	CUF
2C-2C	0.532	86.07	99.9	**0.8617**	25.7
1C-1C	0.684	74.78	99.84	**0.7490**	50.5
0.5C-0.5C	0.802	58.92	100.2	**0.5890**	68.6

B. Real-time Implementation

Simulation are performed for the month of March 2018. Data for the previous month is used to tune the ARMA model. ARMA models takes into account the previous 3 time intervals and 3 previous days, i.e., $D = 3$. Table VI shows the comparison of arbitrage, reactive compensation and peak demand gains for deterministic results with real-time implementations using Algorithm 2. The arbitrage gains are more sensitive to parameter uncertainty for battery with faster ramping battery. The results are in sync with observations made in [38]. The power factor correction gains are not influenced by future parameter uncertainties, as observed in [16]. The peak demand shaving similar to arbitrage gains are affected by parameter uncertainty more significantly for batteries with faster ramping.

TABLE VI
DETERMINISTIC AND REAL-TIME IMPLEMENTATION FOR MARCH 2018

Battery Type	G_{arb}	G_{reac}	G_{peak}	G_T
Deterministic results: **rolling horizon of 1 day**				
0.5C-0.5C	3.723	5.855	4.337	13.914
1C-1C	6.523	5.855	8.674	21.051
2C-2C	10.719	5.855	16.221	32.794
Real-time implementation: **ARMA + MPC**				
0.5C-0.5C	2.819	5.855	4.337	13.010
1C-1C	5.073	5.855	5.590	16.518
2C-2C	9.226	5.855	10.800	25.880

VI. Conclusion

We present an energy storage co-optimization formulation for arbitrage, power factor correction and peak shaving. Despite the different time-scales (minutes to a month) and non-convexity of the optimization problem, the optimization problem can be solved efficiently, and further extended to include battery degradation. Through numerical simulations with realistic battery parameters, real prices for arbitrage and peak demands, we show that total storage gains of the user can be maximized without sacrificing individual optimization gains. Comparing dollars per cycle indicate that faster ramping batteries need not be more profitable for the consumer. We propose an online implementation of the proposed co-optimization formulation using Model Predictive Control. We observe that peak demand and arbitrage gains, but not power factor correction, are sensitive to uncertainties in forecast, with sensitivity being higher for faster ramp rates.

References

[1] N. Li, L. Chen, and S. H. Low, "Optimal demand response based on utility maximization in power networks," in *2011 IEEE power and energy society general meeting*. IEEE, 2011, pp. 1–8.

[2] M. U. Hashmi, D. Muthirayan, and A. Bušić, "Effect of real-time electricity pricing on ancillary service requirements," in *Proceedings of the Ninth International Conference on Future Energy Systems*. ACM, 2018, pp. 550–555.

[3] M. Hashmi, A. Mukhopadhyay, A. Busic, and J. Elias, "Optimal control of storage under time varying electricity prices," in *IEEE International Conference on Smart Grid Communications*, 2017.

[4] R. Walawalkar, J. Apt, and R. Mancini, "Economics of electric energy storage for energy arbitrage and regulation in new york," *Energy Policy*, vol. 35, no. 4, pp. 2558–2568, 2007.

[5] A. Kern, J. Johnson, and J. Mathieu, "Environmental impacts of using energy storage aggregations to provide multiple services," in *Proceedings of the 52nd Hawaii International Conference on System Sciences*, 2019.

[6] "Pjm performance score," Online, https://tinyurl.com/ycq8oqgr, 2016.

[7] s. e. Danielle Croop, Online, https://tinyurl.com/yb795xwb.

[8] K. Bradbury, L. Pratson, and D. Patiño-Echeverri, "Economic viability of energy storage systems based on price arbitrage potential in real-time us electricity markets," *Applied Energy*, vol. 114, pp. 512–519, 2014.

[9] C. Silcox, "Pg&e rates overview," https://www.arb.ca.gov/msprog/asb/workshop/pge.pdf, Aug. 2017.

[10] VCharge, AAU, Route Monkey, CERTH, Prsma, and RINA-C, "Most Appropriate DR Services for each Pilot," EUROPEAN COMMISSION, Bristol, UK, Technical report 5.1, Feb. 2018.

[11] L. Liu, W. Miller, and G. Ledwich, "Solutions for reducing electricity costs for communal facilities. australian ageing agenda," https://tinyurl.com/y5p5gcsu, 2017.

[12] A.-H. Mohsenian-Rad and A. Leon-Garcia, "Optimal residential load control with price prediction in real-time electricity pricing environments," *IEEE Trans. Smart Grid*, vol. 1, no. 2, pp. 120–133, 2010.

[13] A. Oudalov, R. Cherkaoui, and A. Beguin, "Sizing and optimal operation of battery energy storage system for peak shaving application," in *Power Tech, 2007 IEEE Lausanne*. IEEE, 2007, pp. 621–625.

[17] H. Wang *et al.*, "Energy storage for power factor correction in battery charger for electric-powered vehicles," Oct. 16 2014, uS Patent App. 14/139,059.

[14] J. Leadbetter and L. Swan, "Battery storage system for residential electricity peak demand shaving," *Energy and buildings*, vol. 55, pp. 685–692, 2012.

[15] M. Zheng, C. J. Meinrenken, and K. S. Lackner, "Smart households: Dispatch strategies and economic analysis of distributed energy storage for residential peak shaving," *Applied Energy*, vol. 147, pp. 246–257, 2015.

[16] M. U. Hashmi, D. Deka, A. Busic, L. Pereira, and S. Backhaus, "Arbitrage with power factor correction using energy storage," *arXiv preprint arXiv:1903.06132*, 2019.

[18] D. J. Carnovale and A. Barchowsky, "Energy savingsrealistic expectations for commercial facilities," pp. 1–16, 2015.

[19] K. Anderson and A. El Gamal, "Co-optimizing the value of storage in energy and regulation service markets," *Energy Systems*, vol. 8, no. 2, pp. 369–387, 2017.

[20] B. Cheng and W. Powell, "Co-optimizing battery storage for the frequency regulation and energy arbitrage using multi-scale dynamic programming," *IEEE Transactions on Smart Grid*, pp. 1–1, 2016.

[21] S. Sun, B. Liang, M. Dong, and J. A. Taylor, "Phase balancing using energy storage in power grids under uncertainty," *IEEE Transactions on Power Systems*, vol. 31, no. 5, pp. 3891–3903, 2016.

[22] Y. Shi, B. Xu, D. Wang, and B. Zhang, "Using battery storage for peak shaving and frequency regulation: Joint optimization for superlinear gains," *IEEE Trans. on Power Systems*, vol. 33, no. 3, pp. 2882–2894, 2018.

[23] C. D. White and K. M. Zhang, "Using vehicle-to-grid technology for frequency regulation and peak-load reduction," *Journal of Power Sources*, vol. 196, no. 8, pp. 3972–3980, 2011.

[24] J. Cruise and S. Zachary, "The optimal control of storage for arbitrage and buffering, with energy applications," in *Forecasting and Risk Management for Renewable Energy*. Springer, 2017, pp. 209–227.

[25] M. U. Hashmi, L. Pereira, and A. Busic, "Energy storage roles in madeira, portugal: Co-optimizing for arbitrage, self-sufficiency, peak shaving and energy backup," in *IEEE PES Powertech, Milan*, 2019.

[26] M. Rasouli, C. Pache, P. Panciatici, J. Maeght, R. Johari, and R. Rajagopal, "Cloud storage for multi-service battery operation (extended version)," *arXiv preprint arXiv:1906.00732*, 2019.

[27] PLIEGO TARIFARIO, Gerencia Anlisis Tarifario, UTE Uruguay. [Online]. Available: http://tinyurl.com/y5ug28jh

[28] Power Factor Correction Enerdis France. [Online]. Available: https://tinyurl.com/y5dau8a5

[29] J. Peronnet. Power factor correction kvar policy in countries. [Online]. Available: http://engineering.electrical-equipment.org/power-quality/reactive-power-billing-policy-in-countries.html

[30] T. Stetz. German Guidelines and Laws for PV Grid Integration. [Online]. Available: https://tinyurl.com/yyc7dkcw

[31] Pacific Gas and Electric Company Electric Tariff. [Online]. Available: https://tinyurl.com/y554jxrl

[32] Y. Xu and L. Tong, "Optimal operation and economic value of energy storage at consumer locations," *IEEE Transactions on Automatic Control*, vol. 62, no. 2, pp. 792–807, 2016.

[33] G. P. McCormick, "Computability of global solutions to factorable nonconvex programs: Part iconvex underestimating problems," *Mathematical programming*, vol. 10, no. 1, pp. 147–175, 1976.

[34] M. U. Hashmi, W. Labidi, A. Bušić, S.-E. Elayoubi, and T. Chahed, "Long-term revenue estimation for battery performing arbitrage and ancillary services," in *IEEE SmartGridComm*. IEEE, 2018, pp. 1–7.

[35] M. U. Hashmi, "Optimization and control of storage in smart grids," Ph.D. dissertation, L'École Normale Supérieure, 2019.

[36] "Energy prices," Online, http://www.energyonline.com/Data/, 2018.

[37] "Tesla powerwall," Online, https://tinyurl.com/pp6u5g6, 2017.

[38] Y. Chen, M. U. Hashmi, D. Deka, and M. Chertkov, "Stochastic battery operations using deep neural networks," in *IEEE ISGT, NA Washington DC*, 2019.